

Long-time behavior and different shear regimes in quenched binary mixtures

G. Gonnella*

Dipartimento di Fisica, Università di Bari, and INFN, Sezione di Bari, Via Amendola 173, 70126 Bari, Italy

A. Lamura†

Istituto Applicazioni Calcolo, CNR, Via Amendola 122/D, 70126 Bari, Italy

(Received 17 July 2006; published 9 January 2007)

The dependence on applied shear of the morphological and rheological properties of diffusive binary systems after a quench from the disordered state into the coexistence region is investigated. In particular the behavior of the late-time transversal size of domains L_y , and of the maximum of excess viscosity $(\Delta\eta)_M$ is considered. Numerical results show the existence of two regimes corresponding to weak and strong shear separated by a shear rate of the order of $\gamma_c \sim 1/t_D$ where t_D is the diffusive time. L_y and $(\Delta\eta)_M$ behave as $L_y \sim \gamma^{-\alpha}$ and $(\Delta\eta)_M \sim \gamma^\nu$ with $\alpha = \alpha_s = 0.18 \pm 0.02$, $\nu = \nu_s = -2.00 \pm 0.01$ and $\alpha = \alpha_w = 0.25 \pm 0.01$, $\nu = \nu_w = -0.68 \pm 0.04$ in the strong- and weak-shear regimes, respectively. Differently from what was found in systems with fluctuating velocity field, it is confirmed that domains continue to grow at all times.

DOI: 10.1103/PhysRevE.75.011501

PACS number(s): 64.75.+g, 83.50.Ax, 05.70.Ln

I. INTRODUCTION

When a binary mixture is quenched from a disordered state into the coexistence region, domains of the two phases start to form and grow isotropically with power-law behavior. The growth exponent depends on the physical mechanism operating during phase separation, and “universal” behavior is generally observed. For the purely diffusive case, the typical size of domains grows as $L \sim t^{1/3}$ [1].

If, during the phase separation process, a shear flow acts on the system, the above picture changes under many respects. Domains become elongated in the direction of the flow and, if the applied velocity has profile $v_x = \gamma y$ in the x direction (γ is the shear rate), average domain sizes in the flow and shear directions typically verify the relation $L_x \sim \gamma t L_y$ [2]. The morphological evolution is reflected in a peculiar rheological behavior observed in many theoretical [3,4] and experimental [5,6] studies. An excess viscosity has been measured first reaching a maximum, when the domain network is maximally stretched, and then decreasing when, at higher strain, ruptures and breakups occur in the network. Late-time configurations observed in simulations and experiments typically consist of almost parallel stringlike domains, with the value of L_y depending on the shear rate [5,7–9].

An important question for phase separating systems under shear is whether coarsening continues indefinitely, as in the case without flow, or whether a steady state is reached at late times characterized by finite values of the average domain size. The fast growth in the flow direction makes finite-size effects quite relevant also in experimental systems so that it is not easy to answer to the above question. Recent simulations taking into account fluctuations of the velocity field suggest that an asymptotic steady state with finite domain size is stable [10]. This agrees with hydrodynamic scaling analyses predicting a stationary state from the balance

between interfacial and inertial or viscous stresses [9,11]. There is less agreement on the value of the exponent α describing the dependence of L_y on the shear rate ($L_y \sim \gamma^{-\alpha}$). A value between 1/4 and 1/3 is found in experiments [5] and $\alpha = 1/3$ in simulations [9], while, even with some caution, the value $\alpha = 3/4$ is proposed in Ref. [10].

On the other hand, theories in which the velocity field does not fluctuate—e.g., model B [12] with a shear convective term [1]—predict indefinite coarsening when analyzed in the large- N limit [13,14]. These theories can describe polymer melts and blends with large polymerization index [1]. Simulations of these theories give late-time configurations always formed by stringlike domains, and also in this case one could ask about the dependence of the transversal size on the shear rate [8,9].

In this paper we complete our previous studies on the phase separation of a diffusive system in the presence of a fixed velocity profile [2,3]. Even if we do not find evidence of asymptotic steady states, we will see that an exponent α can be defined also in this model. As already suggested in Ref. [7], our results show that two regimes can be clearly observed corresponding to weak and strong shear. The regimes are separated by the value γ_c corresponding to $\gamma_c t_D \approx 1$ where t_D is the diffusion time of the system. Here we describe these regimes in terms of the value of α and of the behavior of the excess viscosity maximum $(\Delta\eta)_M$. An exponent ν can be defined as $(\Delta\eta)_M \sim \gamma^\nu$ [11], and with respect to previous work we clearly see that the two regimes are characterized by different values of α and ν . We find clear evidence of the exponent $\nu = -2$ predicted in the strong-shear regime [15].

The paper is organized as follows. In Sec. II the model is introduced. Section III is devoted to the presentation and discussion of results, and finally some conclusions are drawn in Sec. IV.

II. THE MODEL

We consider the Ginzburg-Landau free energy

*Electronic address: gonnella@ba.infn.it

†Electronic address: a.lamura@ba.iac.cnr.it

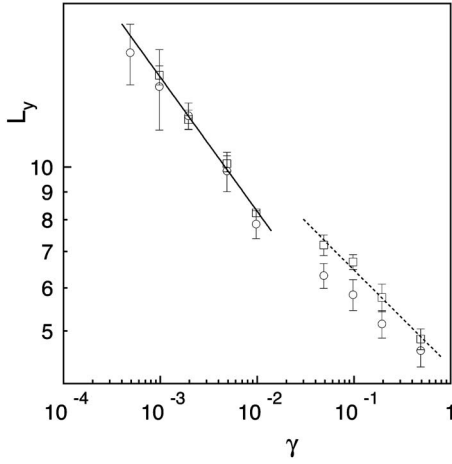


FIG. 1. Log-log plot of the average size L_y of domains along the shear direction at late times as a function of the shear rate γ for two different widths of the system: $W=512$ (\circ) and 1024 (\square). Solid and dashed lines have slopes -0.25 and -0.18 , respectively, and are the best fits to $W=1024$ data. L_y and γ are measured in units of Δx and Δt , respectively.

$$\mathcal{F}\{\varphi\} = \int d^d x \left\{ -\frac{a}{2}\varphi^2 + \frac{b}{4}\varphi^4 + \frac{\kappa}{2}|\nabla\varphi|^2 \right\}, \quad (1)$$

where φ is the order parameter representing the concentration difference between the two components. The polynomial terms in the free-energy density have a single-well structure when $a < 0$, $b > 0$ and describe the disordered state of the mixture with $\varphi_{eq} = 0$. In the ordered state, for $a > 0$, $b > 0$, two symmetric minima are located at $\varphi_{eq} = \pm\sqrt{a/b}$. These are the equilibrium values of the order parameter in the low-temperature limit. The gradient-squared term in Eq. (1) with $\kappa > 0$ takes into account the energy cost of interfaces between domains of different composition. The equilibrium profile between the two coexisting bulk phases can be computed in the one-dimensional case and is $\varphi(x) = \varphi_{eq} \tanh(\frac{2x}{\xi})$, giving [16] a surface tension

$$\sigma = \frac{2}{3}\varphi_{eq}^2\sqrt{2a\kappa} \quad (2)$$

and an interfacial width

$$\xi = 2\sqrt{\frac{2\kappa}{a}}. \quad (3)$$

The thermodynamic properties of the system follow from the free energy (1). The chemical potential difference between the two components is given by

$$\Delta\mu = \frac{\delta\mathcal{F}}{\delta\varphi} = -a\varphi + b\varphi^3 - \kappa\nabla^2\varphi, \quad (4)$$

and the kinetics is described by the convection-diffusion equation

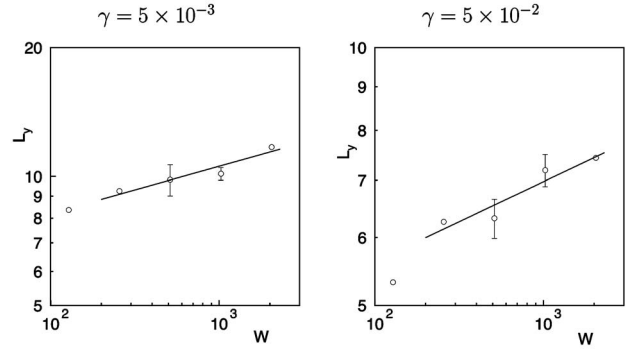


FIG. 2. Log-log plot of the average size L_y of domains along the shear direction at late times as a function of the width W of the system for two different values of the shear rate: $\gamma = 5 \times 10^{-3}$ (left panel) and 5×10^{-2} (right panel). Solid lines have slopes 0.11 and 0.09 in the left and right panels, respectively. L_y and W are measured in units of Δx .

$$\frac{\partial\varphi}{\partial t} + \vec{\nabla} \cdot (\varphi\vec{v}) = \Gamma\nabla^2(\Delta\mu), \quad (5)$$

where the order parameter is coupled to the external velocity field $\vec{v} = \gamma y \vec{e}_x$ with \vec{e}_x the unit vector in the x direction. Γ is a mobility coefficient. When hydrodynamics comes into play a model taking into account also the contribution coming from the Navier-Stokes equation should be used [17].

The only length and time scales of the problem that can be built from macroscopic quantities are ξ and $t_D = \frac{\xi^3\varphi_{eq}^2}{\Gamma\sigma}$ [1,18]. Equation (5) can be cast in a dimensionless form after a redefinition of time, space, and field scales by t_D , ξ , and φ_{eq} , respectively [19]. There is only one dimensionless quantity which appears in the dimensionless equation; it is given by $\bar{\gamma} = \gamma t_D$ which characterizes the strength of the shear flow.

In order to quantify the effect of shear on growth of domains, the average size L_y of domains in the y direction (shear direction) has been computed from the first zero-point crossing of the pair-correlation function. As a check, we also evaluated the domain size in the shear direction from the relation

$$R_y(t) = \pi \frac{\int d\vec{k} C(\vec{k}, t)}{\int d\vec{k} |k_y| C(\vec{k}, t)}, \quad (6)$$

where $C(\vec{k}, t) = \langle \varphi(\vec{k}, t) \varphi(-\vec{k}, t) \rangle$ is the structure factor, with $\varphi(\vec{k}, t)$ being the Fourier transform of the order parameter φ and $\langle \dots \rangle$ denoting an ensemble average.

Of experimental interest are also the rheological indicators, among which the excess viscosity defined as [15,20]

$$\Delta\eta = -\frac{1}{\gamma W^2} \int d\vec{r} \partial_x \varphi \partial_y \varphi, \quad (7)$$

where W is the width of the lattice (the same in all the directions).

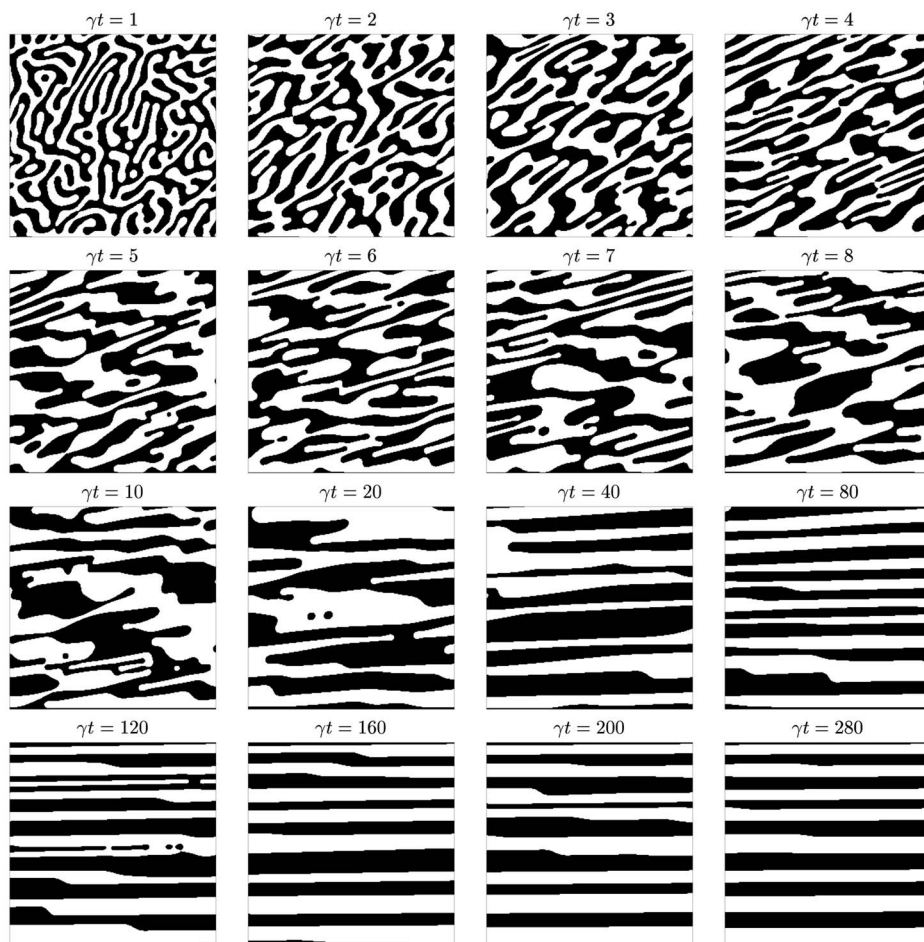


FIG. 3. Sequence at consecutive times of configurations of a portion 256×256 of the whole 1024×1024 system for the case with $\gamma = 5 \times 10^{-3}$.

We have simulated Eq. (5) in two dimensions by a first-order Euler discretization scheme [19] on a regular lattice. Periodic boundary conditions have been implemented in the x direction; Lees-Edwards boundary conditions [21] were used in the y direction. These boundary conditions, originally developed for molecular dynamic simulations of fluids in shear, require the identification of a point at $(x, 0)$ with the one located at $(x + \gamma W \Delta t, W)$, where Δt is the time discretization interval.

III. RESULTS AND DISCUSSION

The system was initialized in a high-temperature disordered state, and the evolution was studied with $a > 0$. Simulations were run using lattices of size $W = 128, 256, 512, 1024, 2048$ with space step $\Delta x = 0.5, 1$. We have not observed significant differences between these two choices of Δx . The results shown here were obtained with γ varying in the range $[5 \times 10^{-4}, 5 \times 10^{-1}]$, $\Delta x = 1$, $\Delta t = 0.01$ for $\gamma \leq 10^{-1}$ and $\Delta t = 0.001$ for $\gamma > 10^{-1}$, $\langle \varphi \rangle = 0$, and averaging over ten independent realizations of the system for each choice of γ and W . We have chosen $\Gamma = a = b = \kappa = 1$. We can then estimate $\xi = 2\sqrt{2}$, $\sigma = 2\sqrt{2}/3$, $\varphi_{eq}^2 = 1$, and $t_D = 24$ in Δx and Δt units. $\bar{\gamma} \approx 1$ corresponds to the value $\gamma_c = 1/t_D \approx 0.04$.

We are interested in studying the behavior of the system at long times ($\gamma t \gg 1$) when configurations are characterized

by stringlike domains along the y direction. We monitored the quantities L_y and R_y , previously defined, which both saturate to a constant value in a single run at fixed γ (see later comments). We used this value to study their dependence on the shear rate γ and on the system size W .

In Fig. 1 we report on a log-log scale the value of L_y as a function of γ for $W = 512, 1024$. We note some main features. The value of L_y depends on the size W of the system and grows as W increases. In the following we will discuss with more details this point. Moreover, the data seem to indicate that a scaling relation $L_y \sim \gamma^{-\alpha}$ holds but with two different exponents for different regions of the shear rate. We tried to fit data points by using a least-squares fit. By fitting all the points together, we found a low correlation coefficient r , so we divided points into two groups. By doing so and using $W = 1024$ data, we found two scaling exponents $\alpha_w = 0.25 \pm 0.01$ with $r_w = -0.997$ for $\gamma \leq 10^{-2}$ and $\alpha_s = 0.18 \pm 0.02$ with $r_s = -0.992$ for $\gamma > 10^{-2}$. Scaling exponents computed by using $W = 512$ data are consistent with the previous ones within error bars, indicating that the scaling exponents are independent of the size of the system. Our data seem then to indicate that the scaling exponents are different in the weak (quantities in this regime are denoted by the subscript w) and in the strong shear (subscript s) regimes, suggesting the existence of a transition at $\gamma_c t_D \approx 1$ between the two regimes. The previous estimate $\gamma_c \approx 4 \times 10^{-2}$ agrees well with numerical results which suggest γ_c to be in the

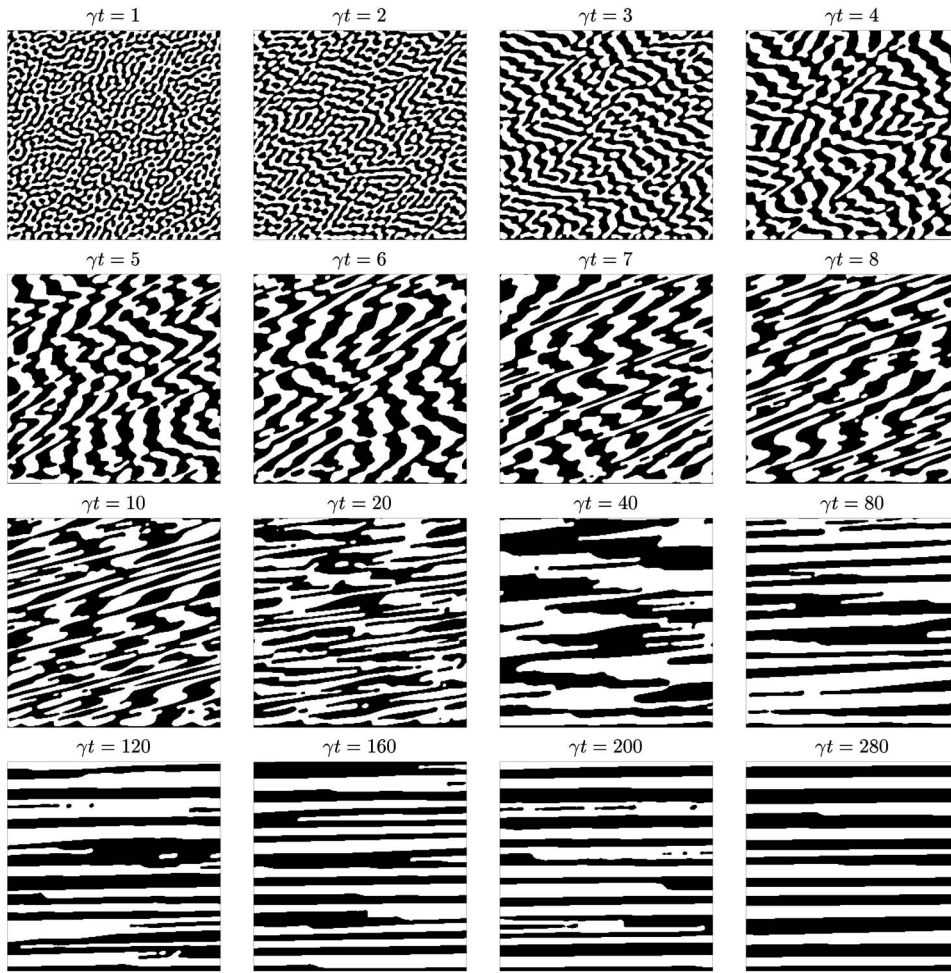


FIG. 4. Sequence at consecutive times of configurations of a portion 256×256 of the whole 1024×1024 system for the case with $\gamma = 5 \times 10^{-2}$.

range $[10^{-2}, 5 \times 10^{-2}]$. All these results are consistent with those obtained using R_y to monitor the size of domains. Former studies without hydrodynamics did not find any indication of such a transition by looking at the transversal size of domains, and the values $\alpha = 0.21 \pm 0.03$ [8] and $\alpha = 0.22 \pm 0.03$ [9] were found. These values are compatible with our results in both regimes within the error bars. A possible reason for the differences we found is that we considered systems with size considerably larger than that ($W = 256$) considered in Ref. [9].

We then turned to investigate the dependence of L_y on the size of the system W by keeping the shear rate fixed. In Fig. 2 we show the plot of L_y as a function of W for two values of γ , one ($\gamma = 5 \times 10^{-3}$) in the weak- and the other ($\gamma = 5 \times 10^{-2}$) in the strong-shear regime. We observe that in both cases L_y grows with W approximately as $L_y \sim W^\beta$. It is a slow growth which seems slightly faster in the weak-shear regime. Best fits give $\beta_w = 0.11 \pm 0.02$ and $\beta_s = 0.09 \pm 0.02$. These results seem to exclude the possibility of an asymptotic steady state; however, they hold only on one decade and are not conclusive. Unfortunately, accessing larger systems becomes quite unfeasible due to required memory and time resources.

So far, we have focused on late-time properties of the systems. Actually, also in preasymptotic kinetics, differences between the weak and strong regimes can be observed. A

typical pattern evolution can be seen in Figs. 3 and 4. Snapshots of a portion 256×256 of a system with size $W = 1024$ are shown at consecutive times for $\gamma = 5 \times 10^{-3}$ and $\gamma = 5 \times 10^{-2}$, respectively. After the usual early stage, when domains are forming from the mixed initial state, a bicontinuous structure is observed. The distortions produced by the flow appear evident from $\gamma t \approx 1$ onward. The higher the shear rate, the larger the anisotropies which appear at a given γt . In the case at lower γ , domains have more time to grow before reaching $\gamma t = 1$ and this is reflected in their average size which is larger compared to the case at higher shear rate. In the meanwhile nonuniformities are formed in the system: Regions with domains of different thickness can be clearly observed. This typical feature of domains with two coexisting different scales along the shear direction was already pointed out in previous studies [2,3]. Small droplets are also present, originating from the fragmentation of strained domains which is more pronounced at a high shear rate. In this latter case domains are more stringlike. This continuous mechanism of stretching and breaking up of domains produces the presence of domains with two typical sizes until patterns are made just of isolated domains completely aligned with the flow direction and the shear acts only to make them smoother. Finally, at the latest times shown, interfaces have become almost completely flat; both the convective and the chemical potential terms in Eq. (5) cannot

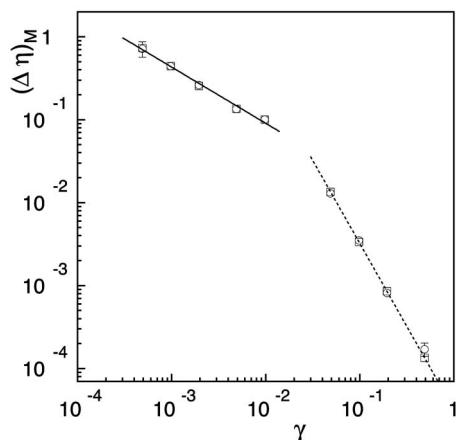


FIG. 5. Log-log plot of the maximum excess viscosity $(\Delta\eta)_M$ as a function of the shear rate γ for two different widths of the system: $W=512$ (\circ) and 1024 (\square). Solid and dashed lines have slopes -0.68 and -2.00 , respectively, and are the best fits to $W=1024$ data. $(\Delta\eta)_M$ is measured in units of Δx , Δt and φ_{eq} , γ in units of Δt .

produce further growth, and the transversal domain size remains constant.

We also computed the excess viscosity $\Delta\eta$ as a function of the strain. After the system is quenched below the critical point, the excess viscosity increases with time, forming two peaks, as already observed in previous studies [3,9,22,23]. The highest peak is located at $\gamma t \approx 2-3$ in the weak-shear regime [9,8,11,13], while its position on the time axis moves rightwards as the shear rate is increased in the strong-shear regime. The time of the peak position in $\Delta\eta$ corresponds to the time when domains are maximally stretched in the flow direction, producing an increase in the effective value of viscosity of the mixture [20]. Subsequent ruptures of domains determine a decrease of $\Delta\eta$. The maximum excess viscosity $(\Delta\eta)_M$ is expected to scale with the shear rate as $(\Delta\eta)_M \sim \gamma^\nu$ with $\nu_w = -2/3$ [11] and $\nu_s = -2$ [15]. Our results for the excess viscosity are shown in Fig. 5 on a log-log scale as a function of the shear rate for two sizes of the system. We do not find any dependence on the size W : Points are well within error bars. The existence of a transition from the weak- to the strong-shear regime located in the range $[10^{-2}, 5 \times 10^{-2}]$ is quite clear and evident here, which is consistent with the results of Fig. 1. Best fits to data points give $\nu_w = -0.68 \pm 0.04$ and $\nu_s = -2.00 \pm 0.01$, in excellent agreement

with theoretical predictions. While the value $\nu_w = -2/3$ has already been found in simulations [8,9], to the best of our knowledge this is the first time that the exponent ν_s is observed.

IV. CONCLUSIONS

In this paper we have considered a phase separating binary mixture under the action of a shear flow. We studied an extension of model B with a convective term induced by the velocity profile $\vec{v} = \gamma y \vec{e}_x$. As previous studies of this system had already shown, late-time configurations typically consist of stringlike domains with the transversal size L_y decreasing for increasing values of γ . The main purpose here was to analyze the dependence of L_y on γ and to look for the existence of different shear regimes.

With our simulations we confirm previous results with continuous growth of domains at all times, as also predicted by the large- N approximation of the model [13,14]. Due to finite-size effects, indefinite growth at asymptotic times can be shown only considering systems with different sizes as we did in the present paper.

Our main finding is that there are two regimes characterized by different values of the exponent α . We checked that these values are stable with respect to the variation of the size of the system. We found $\alpha = 0.18 \pm 0.02$ for $\gamma > \gamma_c$ and $\alpha = 0.25 \pm 0.01$ for $\gamma < \gamma_c$ with $\gamma_c \approx 1/t_D$, t_D being the diffusive time scale for the system. Therefore we see the existence of a different behavior in the weak- and strong-shear regimes. The existence of a transition between weak- and strong-shear regimes appears also in the behavior of the maximum of the excess viscosity $(\Delta\eta)_M$. In Ref. [7] the existence of such a possible transition was found by looking at the behavior of the first normal stress. We found $(\Delta\eta)_M \sim \gamma^\nu$ with $\nu = -2.00 \pm 0.01$ and $\nu = -0.68 \pm 0.04$ in the strong- and weak-shear regimes, respectively. Finally, we observe that actually the whole morphological evolution is influenced by the values of the shear rate. A quantitative analysis of this influence, not presented in the work, could be based on the use of morphological indicators such as Minkowski functionals [24].

ACKNOWLEDGMENT

This work has been partially supported by MIUR (Grant No. PRIN-2004).

[1] K. Binder, in *Phase Transitions in Materials, Materials Science and Technology*, edited by R. W. Cahn, P. Haasen, and E. J. Kramer (VCH, Weinheim, 1990), Vol. 5; H. Furukawa, *Adv. Phys.* **34**, 703 (1985); J. D. Gunton, *et al.*, in *Phase Transitions and Critical Phenomena*, edited by C. Domb and J. L. Lebowitz (Academic, New York, 1983), Vol. 8; A. J. Bray, *Adv. Phys.* **43**, 357 (1994).

[2] F. Corberi, G. Gonnella, and A. Lamura, *Phys. Rev. Lett.* **83**, 4057 (1999).

[3] F. Corberi, G. Gonnella, and A. Lamura, *Phys. Rev. E* **62**, 8064 (2000).

[4] K. Luo and Y. Yang, *Macromol. Theory Simul.* **11**, 429 (2002).

[5] T. Hashimoto, K. Matsuzaka, E. Moses, and A. Onuki, *Phys. Rev. Lett.* **74**, 126 (1995).

[6] W. Gronski, J. Lauger, and C. Laubner, *J. Mol. Struct.* **383**, 23 (1996).

[7] R. Yamamoto and X. C. Zeng, *Phys. Rev. E* **59**, 3223 (1999).

- [8] H. Liu and A. Chakrabarti, *J. Chem. Phys.* **112**, 10582 (2000).
- [9] Z. Shou and A. Chakrabarti, *Phys. Rev. E* **61**, R2200 (2000).
- [10] P. Stansell, K. Stratford, J.-C. Desplat, R. Adhikari, and M. E. Cates, *Phys. Rev. Lett.* **96**, 085701 (2006).
- [11] T. Ohta, H. Nozaki, and M. Doi, *Phys. Lett. A* **145**, 304 (1990); *J. Chem. Phys.* **93**, 2664 (1990).
- [12] P. C. Hohenberg and B. I. Halperin, *Rev. Mod. Phys.* **49**, 435 (1977).
- [13] F. Corberi, G. Gonnella, and A. Lamura, *Phys. Rev. Lett.* **81**, 3852 (1998).
- [14] N. P. Rapapa and A. J. Bray, *Phys. Rev. Lett.* **83**, 3856 (1999).
- [15] A. Onuki, *Phys. Rev. A* **35**, 5149 (1987).
- [16] J. S. Rowlinson and B. Widom, *Molecular Theory of Capillarity* (Clarendon Press, Oxford, 1982).
- [17] A review on the influence of hydrodynamic effects on scaling properties is presented in J. M. Yeomans, *Annu. Rev. Comput. Phys.* **7**, 61 (1999); For simulations with hydrodynamic models, see M. E. Cates, V. M. Kendon, P. Bladon, and J.-C. Desplat, *Faraday Discuss.* **112**, 1 (1999); V. M. Kendon, J.-C. Desplat, P. Bladon, and M. E. Cates, *Phys. Rev. Lett.* **83**, 576 (1999); V. M. Kendon, M. E. Cates, I. Paganobarraga, J.-C. Desplat, and P. Bladon, *J. Fluid Mech.* **440**, 147 (2001); M. E. Cates, J.-C. Desplat, P. Stansell, A. J. Wagner, K. Stratford, I. Paganobarraga, and R. Adhikari, *Philos. Trans. R. Soc. London, Ser. A* **363**, 1917 (2005); A. J. Wagner and J. M. Yeomans, *Phys. Rev. Lett.* **80**, 1429 (1998); *Phys. Rev. E* **59**, 4366 (1999); A. Lamura and G. Gonnella, *Physica A* **294**, 295 (2001).
- [18] A. Frischknecht, *Phys. Rev. E* **56**, 6970 (1997).
- [19] T. M. Rogers, K. R. Elder, and R. C. Desai, *Phys. Rev. B* **37**, 9638 (1988).
- [20] A. Onuki, *J. Phys.: Condens. Matter* **9**, 6119 (1997).
- [21] A. W. Lees and S. F. Edwards, *J. Phys. C* **5**, 1921 (1972).
- [22] Z. Zhang, H. Zhang, and Y. Yang, *J. Chem. Phys.* **113**, 8348 (2000).
- [23] J. Lauger, C. Laubner, and W. Gronski, *Phys. Rev. Lett.* **75**, 3576 (1995).
- [24] K. R. Mecke and V. Sofonea, *Phys. Rev. E* **56**, R3761 (1997).